




## Tear Dynamics in Healthy and Dry Eyes

Colin F. Cerretani & C. J. Radke


To cite this article: Colin F. Cerretani & C. J. Radke (2014) Tear Dynamics in Healthy and Dry Eyes, Current Eye Research, 39:6, 580-595, DOI: [10.3109/02713683.2013.859274](https://doi.org/10.3109/02713683.2013.859274)

To link to this article: <https://doi.org/10.3109/02713683.2013.859274>


 View supplementary material [↗](#)

 Published online: 06 Feb 2014.

 Submit your article to this journal [↗](#)

 Article views: 568

 View Crossmark data [↗](#)

 Citing articles: 19 View citing articles [↗](#)

ORIGINAL ARTICLE

# Tear Dynamics in Healthy and Dry Eyes

Colin F. Cerretani<sup>1</sup> and C. J. Radke<sup>1,2</sup>

<sup>1</sup>Department of Chemical and Biomolecular Engineering, University of California, Berkeley, CA, USA and  
<sup>2</sup>Vision Science Group, University of California, Berkeley, CA, USA

## ABSTRACT

**Purpose:** Dry-eye disease, an increasingly prevalent ocular-surface disorder, significantly alters tear physiology. Understanding the basic physics of tear dynamics in healthy and dry eyes benefits both diagnosis and treatment of dry eye. We present a physiological-based model to describe tear dynamics during blinking.

**Materials and methods:** Tears are compartmentalized over the ocular surface; the blink cycle is divided into three repeating phases. Conservation laws quantify the tear volume and tear osmolarity of each compartment during each blink phase. Lacrimal-supply and tear-evaporation rates are varied to reveal the dependence of tear dynamics on dry-eye conditions, specifically tear osmolarity, tear volume, tear-turnover rate (TTR), and osmotic water flow.

**Results:** Predicted periodic-steady tear-meniscus osmolarity is 309 and 321 mOsM in normal and dry eyes, respectively. Tear osmolarity, volume, and TTR all match available clinical measurements. Osmotic water flow through the cornea and conjunctiva contribute 10 and 50% to the total tear supply in healthy and dry-eye conditions, respectively. TTR in aqueous-deficient dry eye (ADDE) is only half that in evaporative dry eye (EDE).

**Conclusions:** The compartmental periodic-steady tear-dynamics model accurately predicts tear behavior in normal and dry eyes. Inclusion of osmotic water flow is crucial to match measured tear osmolarity. Tear-dynamics predictions corroborate the use of TTR as a clinical discriminator between ADDE and EDE. The proposed model is readily extended to predict the dynamics of aqueous solutes such as drugs or fluorescent tags.

**Keywords:** Blink cycle, dry eye, mathematical model, tear dynamics, tear osmolarity

## LIST OF SYMBOLS

| Variable                       | SI, Common units | Description  |
|--------------------------------|------------------|--|
| $A_{cn}$ , $A_{cj}$ , $A_{pa}$ | $m^2$ , $cm^2$   | Exposed surface area of the cornea, conjunctiva, palpebral aperture      |
| $c$ (C)                        | $mol/m^3$ (mOsM) | Concentration (osmolarity) of salt in . . .                              |
| $c_\alpha$                     | "                | . . .compartment $\alpha$  |
| $c_j$ , $c_k$                  | "                | . . .stream $j$ or $k$ entering or leaving compartment $\alpha$          |
| $c_{lac}$                      | "                | . . .tear secreted from lacrimal gland                                   |
| $c_{im}$                       | "                | . . .meniscus $i = u$ or $l$ for upper or lower                          |
| $c_{si}$                       | "                | . . .stream entering meniscus $i = u$ or $l$ for upper or lower          |
| $c_{tf}$ , $c_{tf,max}$        | "                | . . .the tear film, maximum salt concentration in tear film              |
| $c(x,t)$                       | "                | . . .conjunctival sac as a function of $x$ and $t$                       |
| $c_{\alpha F}$                 | "                | . . .compartment $\alpha$ at end of interblink                           |
| $c_b$ ( $C_b$ )                | "                | Bulk salt concentration (osmolarity) after mixing                        |
| $c_{b,it}$                     | "                | $c_b$ of a given iteration during <i>Regula-Falsi</i> numerical solution |

(continued)

Received 3 May 2013; revised 9 September 2013; accepted 21 October 2013; published online 6 February 2014

Correspondence: Professor Clayton J. Radke, PhD, Department of Chemical and Biomolecular Engineering, University of California, Berkeley, 101E Gilman Hall, Berkeley, CA 94720, USA. Tel: +1 510 642 5204. Fax: +1 510 642 4778. E-mail: radke@berkeley.edu

| Variable                       | SI, Common units                          | Description  |
|--------------------------------|---|--|
| $C_D, C_D(0)$                  | mol/m <sup>3</sup>                        | Concentration of dye in tear, initial $C_D$ upon instillation  |
| $CS, CS_0, CS_{tf}$            |   | Control surface of upper meniscus during deposition, $0$ and $tf$ denote the superior and inferior surfaces over which tear fluid enters and exits |
| $CV$                           |   | Control volume of upper meniscus during deposition   |
| $h_0$                          | m, $\mu$ m                                | Distance between upper lid and ocular surface during deposition  |
| $h_c$                          | m, $\mu$ m                                | Thickness of tear fluid in the conjunctival sacs   |
| $h_{tf}$                       | m, $\mu$ m                                | Tear-film thickness  |
| $\langle h_{tf} \rangle$       | m, $\mu$ m                                | Time-average initially deposited tear-film thickness   |
| $h_{pa}$                       | m, $\mu$ m                                | Palpebral-aperture height  |
| $i$                            |   | Subscript index denoting upper ( $u$ ) or lower ( $l$ )  |
| $j$                            |   | Subscript index denoting $j$ -th stream entering compartment $\alpha$  |
| $J_e$                          | m/s, $\mu$ m/min                          | Volumetric evaporative water flux  |
| $J_w, J_{w,n}$                 | m/s, $\mu$ m/min                          | Volumetric osmotic water flux through cornea or conjunctiva ( $n = cn$ or $cj$ )   |
| $J, K$                         |   | Total number of entering ( $J$ ) or exiting streams ( $K$ ) in compartment $\alpha$  |
| $k$                            |   | Subscript index denoting $k$ -th stream exiting compartment $\alpha$   |
| $L_{ic}$                       | m, $\mu$ m                                | Average depth of fornix $i = u$ (upper) or $l$ (lower)   |
| $\underline{n}$                |   | Outward-pointing unit normal for control surface $CS$  |
| $\bar{P}_{cn}, P_{cj}$         | m/s                                       | Corneal ( $cn$ ) and conjunctival ( $cj$ ) osmotic water permeability  |
| $q$                            | m <sup>3</sup> /s, $\mu$ L/min            | Volumetric water flow rate...  |
| $q_0$                          | "   | ...into the upper meniscus from the conjunctival sac during  |
| deposition                     | "   | ...due to osmotic flow into the conjunctival sacs  |
| $q_c$                          | "   | ...due to osmotic flow through the cornea  |
| $q_{cn}$                       | "   | ...due to osmotic flow into the tear film  |
| $q_{ctf}$                      | "   | ...of all combined osmotic water flows   |
| $q_{cT}$                       | "   | ...from drainage through both puncta, or from punctum $i = u$ or $l$   |
| $q_{dr}, q_{di}$               | "   | ...from evaporation from all surfaces, or from meniscus $i = u$ or $l$   |
| $q_{ev}, q_{ei}$               | "   | ...in stream $J$ ( $j$ ) or $K$ ( $k$ ) entering or exiting compartment $\alpha$   |
| $q_j, q_k$                     | "   | ...from the lacrimal supply into the conjunctival sacs   |
| $q_{lac}$                      | "   | ...maximum drainage volumetric flow rate from each meniscus  |
| $q_m$                          | "   | ...from conjunctival sac $i$ into meniscus $i$ during interblink   |
| $q_{si}$                       | "   | Eye-globe radius   |
| $R$                            | m, cm                                     | Minimum meniscus radius for drainage   |
| $R_0$                          | m, $\mu$ m                                | Upper- and lower-meniscus radii at beginning of deposition   |
| $R_b$                          | m, $\mu$ m                                | Radius of meniscus $i = u$ or $l$  |
| $R_{im}$                       | m, cm                                     | Lid-margin perimeter for a single lid  |
| $S_{iid}$                      | m, cm                                     | Time   |
| $t$                            | s   | Duration of the closure phase  |
| $t_c$                          | s   | Duration of the deposition phase   |
| $t_d$                          | s   | Duration of the interblink phase   |
| $t_{ib}$                       | s   | Characteristic time for clearance of conjunctival sac $i = u$ or $l$   |
| $t_{ci}$                       | s   | Tear-turnover rate   |
| TTR                            | %/s, %/min                                | Fluid velocity entering control surface $CS$   |
| $\underline{u}$                | m/s                                       | Average fluid velocity entering conjunctival sac at $x = 0$  |
| $u_{lac}$                      | m/s                                       | Linear velocity of rising upper lid during deposition  |
| $U$                            | m/s, cm/s                                 | Specific volume of water   |
| $v_w$                          | m <sup>3</sup> /mol, cm <sup>3</sup> /mol | Volume of compartment $\alpha$ , at the end of interblink  |
| $V_{\alpha}$ or $V_{\alpha F}$ | m <sup>3</sup> , $\mu$ L                  | Volume of meniscus $i = u$ or $l$  |
| $V_{im}$                       | "   | Total tear volume as measured by fluorescent dilution  |
| $V_t$                          | "   | Total model tear volume, at beginning of deposition ( $D$ ) or end of interblink ( $F$ )   |
| $V_T, V_{TD}, V_{TF}$          | "   | Tear-film volume   |
| $V_{tf}$                       | "   | Distance along conjunctival sac beginning from the apex of the fornix  |
| $x$                            | m, $\mu$ m                                | Subscript index denoting compartment   |
| $\alpha$                       |   | Mixing parameter for conjunctival sac $i$  |
| $\beta_i$                      |   | Characteristic ratio from Equations (B.9–10)   |
| $\gamma$                       |   | Beginning ( $\theta_1$ ) and end ( $\theta_2$ ) positions of palpebral aperture  |
| $\theta_1, \theta_2$           | rad                                       | Angular medial-lateral width of palpebral aperture   |
| $\theta_A$                     | rad                                       | Tear-turnover rate in min <sup>-1</sup>  |
| $\kappa$                       | s <sup>-1</sup> , min <sup>-1</sup>       | Fraction of total lacrimal secretion directed to conjunctival sac $i$  |
| $\lambda_i$                    |   | Tear viscosity   |
| $\mu$                          | Pa·s, cP                                  | Tear density   |
| $\rho$                         | kg/m <sup>3</sup> , g/cm <sup>3</sup>     | Tear surface tension   |
| $\rho$                         | N/m, mN/m                                 | Angular superior-inferior height of palpebral aperture   |
| $\sigma$                       |   | Lid-opening angular velocity during deposition   |
| $\varphi_A$                    | rad                                       |  |
| $\omega$                       | rad/s                                     |  |

## INTRODUCTION

Dry eye, one of the most common ocular-surface disorders, may affect as much as 30% of the worldwide population.<sup>1</sup> The International Dry Eye Workshop<sup>2</sup> (DEWS) defines dry eye as *a multifactorial disease of the tears and ocular surface that results in symptoms of discomfort, visual disturbance, and tear film instability. It is accompanied by increased osmolarity of the tear film and inflammation of the ocular surface.* The role of increased tear osmolarity (salinity) in dry eye was suspected by early investigators<sup>3-5</sup>, but not proven convincingly until 1978 by Gilbard.<sup>6,7</sup> More than 30 years later, enhanced osmolarity remains central to the definition of dry eye.<sup>2</sup> Because tear hyperosmolarity repeatedly correlates with both the presence and severity of dry eye,<sup>8,9</sup> it has been suggested as the single most effective marker of dry eye.<sup>10-12</sup>

Tear bathing the ocular surface contains dissolved salts, proteins, and mucins, and is produced as an isotonic fluid by the main and accessory lacrimal glands of the eye.<sup>13</sup> Water evaporates from the exposed 3-to-5- $\mu\text{m}$  thick tear film between blinks, thereby concentrating salts. Whereas the measured tear osmolarity for healthy individuals is near 300 milli-Osmoles per liter (mOsM), it can reach up to 400 mOsM for dry-eye sufferers.<sup>6,7,9,11,12</sup> Increased tear evaporation and decreased tear supply both amplify this effect; dry eye resulting from these two stimuli is termed, respectively, evaporative dry eye (EDE) and aqueous-deficient dry eye (ADDE).

Increased evaporation typically originates from lid diseases, such as meibomian gland dysfunction (MGD), that compromise the tear-film lipid layer (TFLL) or from arid or windy environments.<sup>14-19</sup> Deficient lacrimal-tear production is commonly a result of aging or of Sjögrens syndrome.<sup>2</sup> Resulting tear hyperosmolarity decreases mucin expression and triggers a proinflammatory signaling cascade that leads to tear instability, inflammation, and epithelial cell death.<sup>20</sup> It is currently understood that these stressors exacerbate each other, perpetuating a vicious cycle of inflammation and ocular-surface damage that is dry eye.<sup>20, 21</sup>

Increased tear-evaporation rate and decreased tear-supply rate both correlate experimentally with increased tear osmolarity and dry-eye disease.<sup>2</sup> Thus, tear-flow dynamics is fundamental to dry eye. Development of a mechanistic quantitative relationship between tear dynamics and tear osmolarity, however, is difficult to accomplish experimentally. Simultaneous tracking of salt and water flows over the ocular surface while also measuring tear flow and evaporation rates is impractical. Continuum modeling of tear dynamics relates tear flows to tear osmolarity, and enables interrogation of tear behavior over a wide range of tear-evaporation and tear-supply rates not readily assessed in the clinic.

Based on their study of corneal and conjunctival water permeability, Levin and Verkman<sup>22</sup> were the first to develop a simple mathematical model to predict tear osmolarity in mouse eyes. They assumed that the tears occupy a single, well-mixed compartment, and they accounted for tear evaporation, lacrimal secretion, and osmotically driven water flow through the ocular surface. For normal tear-evaporation and lacrimal-supply rates, analytical solution predicted a normal tear osmolarity approximately 7 mOsM above isotonic. In agreement with clinical observations, they found that increased evaporation, decreased lacrimal secretion, and decreased osmotic flow resulted in elevated tear osmolarity.

Zhu and Chauhan published several papers modeling tear drainage,<sup>23</sup> mixing,<sup>24</sup> osmolarity, and volume.<sup>25,26</sup> Their improved calculations incorporated not only the physics of tear deposition and drainage, but also detailed biological models of salt and water transport through the conjunctival epithelia, allowing them to predict total tear volume and osmolarity. They calculated a normal tear osmolarity of 298 mOsM, significantly less than their assumed 362 mOsM for the lacrimal-supply osmolarity. Active and passive water and solute transport through the conjunctiva played an important role in the predicted tear osmolarity and tear flow. Simplification of the tear compartmentalization over the ocular surface and absence of inter-compartmental blink dynamics prevented analysis of solute distribution across the eye.

Tears are not continuous over the ocular surface, but are distributed into different regions including the lid margins, the precorneal tear film, and the conjunctival sacs (fornices). Different regions exhibit distinct tear volumes<sup>27,28</sup> and are not continuous with each other. That is, it takes time for fluid and solute to mix between regions.<sup>29,30</sup> Therefore, the salt concentration varies between regions depending on local dynamics. Because osmolarity initiates both ocular-surface damage and transmembrane water transport through the epithelia, details of salt and water exchange in each compartment must be addressed.

The recent work of Gaffney et al.<sup>31</sup> accounted for tear compartmentalization, and represents a significant improvement as it describes the osmolarity difference between the meniscus and the tear film. The perched tear film experiences tear evaporation that significantly concentrates the remaining fluid because it is hydraulically isolated from the menisci by the black lines.<sup>32,33</sup> This result is of particular importance because clinically reported tear osmolarities are almost always obtained by sampling from the lower meniscus, whereas the osmolarity experienced by the epithelial cells in most of the palpebral aperture is considerably higher.<sup>31,34</sup> For a normal individual, a tear osmolarity of 313 mOsM was predicted by Gaffney et al., 11 mOsM higher than the lacrimal secretion osmolarity. Gaffney et al.

investigated tear behavior (i.e. transient compartment volumes and osmolarities) over a range of tear-evaporation rates, lacrimal-supply rates, blink frequencies, and inter-compartmental mixing schemes. They describe tear dynamics for EDE and ADDE, and discuss the effectiveness of blink-rate increases in combating dry eye-induced tear hyperosmolarity. Many tear fluxes and geometries, however, are estimated for the normal case only, decoupling the interblink dynamics from deposition and drainage physics. Additionally, Gaffney et al. do not include water flow through the ocular epithelial surfaces. Consequently, their results are limited to low tear-evaporation rates and to high lacrimal-supply rates in order to obtain normal tear osmolarity.

We couple the physics of tear-film deposition, tear drainage, water and solute distribution, and osmotic-driven water flow through the cornea and conjunctiva. Although our effort shares similar assumptions to those of Gaffney et al.,<sup>31</sup> we consider only the periodic-steady-state behavior of the tears. In addition, inclusion of osmotic water flow through the conjunctival and corneal epithelia enables matching to a wider range of clinically reported tear measurements and highlights the role of conjunctival and corneal water secretion in maintaining tear osmolarity. In dry-eye conditions, we find that the osmotic water-flow rate through the cornea and conjunctiva can be as much as half of the lacrimal-supply rate.

Predicted results are compared to important clinical tear measurements including tear production, tear-turnover rate (TTR), tear volume, tear-film thickness, and tear osmolarity. By treating the lacrimal-supply and tear-evaporation rates as parameters,

we predict tear dynamics for a wide range of conditions, primarily those of dry eye. Comparison to clinical measurements generates insight into the differences in tear dynamics between normal, ADDE, and EDE subjects and corroborates use of TTR as a clinical discriminator between ADDE and EDE. We also examine the ramifications of the highest measured tear-film thinning rates<sup>35,36</sup> on tear osmolarity. These high evaporation rates give rise to tear osmolarities well above those measured in dry-eye conditions.

## MODEL DESCRIPTION

Tear dynamics describes the distribution and flow of water through and over the ocular surface. Based on tear physiology, we divide tears into five distinct compartments and perform water and salt balances on each compartment to yield tear volumes and salt concentrations for each. Periodic-steady transient changes in salt concentration and tear volume are predicted within individual compartments over repeating blink cycles. Figure 1 shows sagittal cross-sections of the apical anterior eye and lids during the three phases of the blink cycle: tear deposition that starts as the upper lid rises; interblink, during which the eye remains open; and closure, which occurs as the upper lid falls. Volumetric tear-flow rates during interblink are indicated by the symbol  $q$  [ $\text{m}^3/\text{s}$ ]. After closure, the cycle begins anew, repeating identically: a periodic-steady state emerges. We describe below the tear compartmentalization and geometries, the water and salt balances for each compartment during each

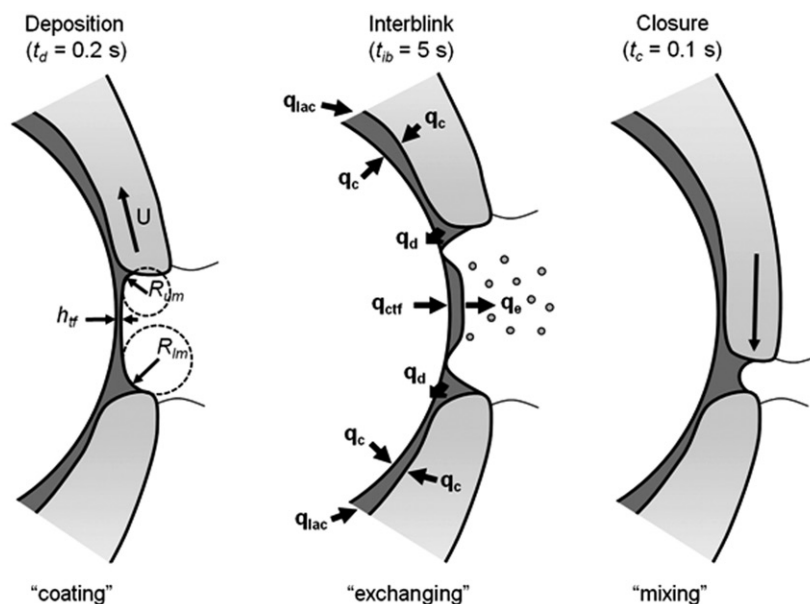


FIGURE 1 Schematic sagittal view of the apical anterior eye and lids including tear film thickness  $h_{tf}$ . The blink cycle is divided into three phases that repeat continuously: deposition, interblink, and closure. Water-flow streams are indicated by arrows labeled with pertinent volumetric flow rates  $q$ .



TABLE 1 Model parameters for “normal” individual.

| Parameter                                      | Symbol      | Value (common)       | (SI units)                              | Source(s)                            |
|--|-------------|----------------------|---|--------------------------------------|
| Eye-globe radius                               | $R$         | 1.2 cm               | 0.012 m                                 | 69,70                                |
| Palpebral-aperture height                      | $h_{pa}$    | 9.0 mm               | 0.009 m                                 | 27,62,71                             |
| Palpebral-aperture area                        | $A_{pa}$    | 2.1 cm <sup>2</sup>  | $2.1 \times 10^{-4}$ m <sup>2</sup>     | 27,60,62                             |
| Lid-margin perimeter                           | $S_{lid}$   | 30 mm                | 0.03 m                                  | 27                                   |
| Upper-fornical area                            | $A_{uf}$    | 3.8 cm <sup>2</sup>  | $3.8 \times 10^{-4}$ m <sup>2</sup>     | Geometry, <sup>72</sup>              |
| Lower-fornical area                            | $A_{lf}$    | 2.7 cm <sup>2</sup>  | $1.7 \times 10^{-4}$ m <sup>2</sup>     | Geometry, <sup>72</sup>              |
| Total conjunctival area                        | $A_{conj}$  | 14.1 cm <sup>2</sup> | $14.1 \times 10^{-4}$ m <sup>2</sup>    | Calculation                          |
| Center lid-opening velocity                    | $U$         | 5 cm/s               | 0.05 m/s                                | Calculation, <sup>46</sup>           |
| Deposition time                                | $t_d$       | 0.18 s               | 0.18 s                                  | Calculation, <sup>46</sup>           |
| Interblink time                                | $t_{ib}$    | 5.0 s                | 5.0 s                                   | 69                                   |
| Secreted-tear osmolarity                       | $c_{lac}$   | 300 mOsM             | 150 mol/m <sup>3</sup>                  | 39                                   |
| Tear viscosity                                 | $\mu$       | 1.5 cP               | 0.0015 Pa·s                             | 73                                   |
| Tear surface tension                           | $\sigma$    | 45 mN/m              | 0.045 N/m                               | 74                                   |
| Tear mass density                              | $\rho$      | 1 g/cm <sup>3</sup>  | 10 <sup>3</sup> kg/m <sup>3</sup>       |                                      |
| Lid-ocular surface gap thickness               | $h_0$       | 2 μm                 | $2.0 \times 10^{-6}$ m                  | Estimated                            |
| Conjunctival-sac thickness                     | $h_c$       | 7.0 μm               | $7.0 \times 10^{-6}$ m                  | 27,38                                |
| Conjunctival water permeability                | $P_{cj}$    | 0.00125 cm/s         | $1.25 \times 10^{-5}$ m/s               |                                      |
| Corneal water permeability                     | $P_{cn}$    | 0.00125 cm/s         | $1.25 \times 10^{-5}$ m/s               |                                      |
| Maximum drainage rate                          | $q_m$       | 1.0 μL/min           | $2.8 \times 10^{-11}$ m <sup>3</sup> /s | Based on Zhu & Chauhan <sup>23</sup> |
| Minimum drainage radius                        | $R_0$       | 120 μm               | $1.2 \times 10^{-4}$ m                  | Based on Zhu & Chauhan <sup>23</sup> |
| Mixing fraction in conjunctival sac            | $\beta_i$   | 1.0                  | 1.0                                     |                                      |
| Fraction of $q_{lac}$ directed to upper fornix | $\lambda_u$ | 0.80                 | 0.80                                    | 75                                   |
| Healthy lacrimal tear-secretion rate           | $q_{lac}$   | 1.10 μL/min          | $2.1 \times 10^{-11}$ m <sup>3</sup> /s | 43                                   |
| Healthy tear-evaporation rate                  | $q_e$       | 0.15 μL/min          | $1.2 \times 10^{-12}$ m <sup>3</sup> /s | 43                                   |

blink phase, parameter estimation, and finally the numerical method to solve the resulting coupled nonlinear ordinary differential equations. Chosen values for compartment geometries (Appendix A of Supplementary Material), tear physical properties, and other required parameters are listed in Table 1.

### Tear Flow and Compartments

The leftmost panel in Figure 1 shows the tear-deposition phase as the upper lid rises at velocity  $U$  to leave behind the aqueous tear film over the exposed ocular surface.<sup>37</sup> The upper and lower menisci radii are labeled  $R_{um}$  and  $R_{lm}$ , respectively. The lower meniscus remains static while the upper-meniscus volume shrinks due to loss of fluid to the deposited tear film. The tear-film thickness,  $h_{tf}$ , is proportional to  $R_{um}$ .<sup>37</sup> More tear in the upper meniscus increases  $h_{tf}$ . As the upper lid rises, some tear is uncovered behind the meniscus, partially replenishing the upper-meniscus volume. At the end of the 0.2-s deposition phase, the upper-meniscus radius is smaller than that of the lower meniscus due to fluid loss to the tear film.

Within 0.03 s of lid opening, capillary forces locally thin the tear film immediately adjacent to the lid menisci to form the black lines originally observed by McDonald and Brubaker.<sup>32,33,37</sup> These deep channels pinch off the tear film, isolating it from the bordering menisci. Consequently, the central panel in Figure 1 partitions the exposed tears during an interblink into three compartments: the upper and lower menisci that

lie along the lid margins and the perched precorneal tear film that coats the exposed cornea and conjunctiva.<sup>27,38</sup> Essentially no water or solute exchange occurs between the menisci and the perched tear film.<sup>32,33</sup> Conjunctival sacs behind the upper and lower lids also serve as reservoirs for tear fluid. These five regions, shown in Figure 2, define the five tear compartments of the model.

The majority of tear flow occurs during interblink. Aqueous tear originates as a nearly isotonic mixture of water, salt, and proteins.<sup>39</sup> Tear produced in the main and accessory lacrimal glands enters the base of the upper and lower conjunctival sacs at a combined volumetric flow rate  $q_{lac}$ .  $\lambda_u$  and  $\lambda_l$  quantify the fractions of the total lacrimal supply that enter the upper and lower conjunctival sacs, respectively. Osmotically driven water flow through the palpebral and bulbar conjunctivae, labeled  $q_c$ , enhances tear flow in the conjunctival sacs where osmolarity is elevated above isotonic. Experiments utilizing radioactive tracer (scintigraphy)<sup>29</sup> and fluorescein dye<sup>30</sup> demonstrate that solutes instilled in the conjunctival sacs eventually reach the precorneal tear film by mixing and flow. Thus, lacrimal-secreted tear reaches the lid margin and enters the menisci.

In the exposed tear, small particles placed in the menisci flow laterally along the lid margin towards the puncta before draining into the canaliculi, but do not flow into the isolated tear film during interblink.<sup>38</sup> Thus, tear from the conjunctival sacs enters the superior and inferior menisci from which it is lost via punctal drainage or evaporation. Evaporative loss from the menisci is minimal. However, the large

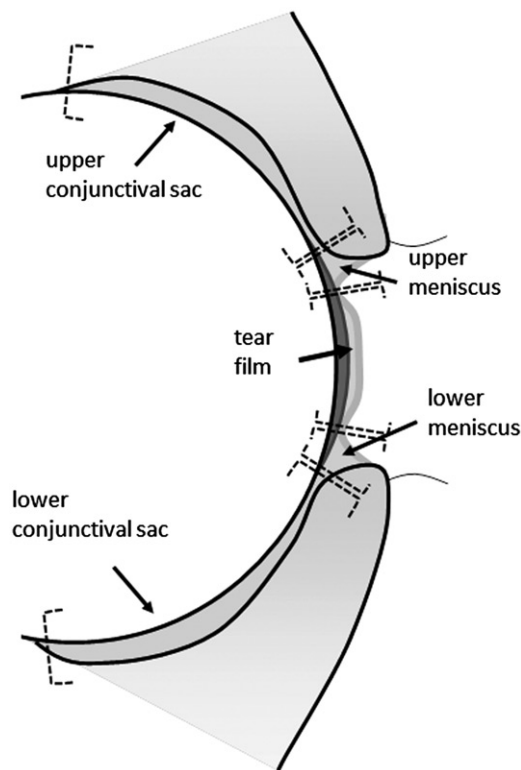


FIGURE 2 Schematic sagittal view of the apical anterior eye during interblink. The five tear compartments are defined by opposing dotted brackets. Drawing is not to scale.

surface area of the perched tear film results in significant water loss,  $q_e$  in Figure 1. Similar to the conjunctival sacs, water enters or exits the tear film via osmotic flow through the cornea and conjunctiva, labeled  $q_{ctf}$ . Gradients in hydraulic pressure, osmotic pressure, and electrical potential drive water flow between the tears and blood serum through the conjunctiva or between the tears and aqueous humor through the cornea. As with many biological membranes, water transport through these tissues occurs through a complex combination of passive and active transport.<sup>40</sup> Detailed descriptions of coupled ion and water transport have been worked out for both the cornea and conjunctiva.<sup>26,41</sup> We approximate water flow through the palpebral and bulbar conjunctivae as osmotic-driven flow characterized solely by the water permeability of the membrane  $P_{cj}$  [m/s] and the osmotic concentration difference between the tears and serum, similar to Levin and Verkman.<sup>22</sup> To describe transcorneal water flow, we utilize the results of Leung et al.<sup>41</sup> for water flow through the cornea,  $q_{cnr}$  versus tear osmolarity as described previously by Cerretani et al.<sup>42</sup>

After interblink, the upper lid descends toward the lower lid, initiating the closure phase, which lasts about 0.1 s. During closure, shown in the rightmost panel of Figure 1, tear originating from the various compartments mixes. Tear in the exposed

compartments mixes completely. The extent of fluid mixing in the tear of the conjunctival sacs during a normal blink, however, is unclear. Under controlled gaze in a scintigraphy study,<sup>29</sup> tracer inserted in the menisci rarely traveled back under the lids. Nevertheless, most current fluorescence studies rely on the observation that fluorescent dye placed in upper and lower conjunctival sacs dilutes over the total tear volume after forceful blinking.<sup>27,43–45</sup> The difference in mixing behavior is likely due to differences in blink strength and eye movement. We hypothesize that complete mixing of the exposed tear with unexposed tear may not occur with every blink, but over a long time period, tear is effectively mixed.

At the end of closure, the upper lid rises, commencing the deposition phase. A new blink cycle begins. Within one transient blink cycle, compartment volumes and salt concentrations vary, but they repeat identically after each blink cycle. Thus, tear dynamics follows a periodic-steady state.

### Water and Salt Balances

To predict compartment volumes and osmolarities in the periodic-steady state, we conserve the mass of water and salt that enters or exits each compartment during each phase of the blink cycle. Upon neglecting water-density variation due to dilute salts present in the tears, water volumes must balance in each of the five compartments

$$\frac{dV_\alpha}{dt} = \sum_j^J (q_j)_{in} - \sum_k^K (q_k)_{out} \quad (1)$$

where  $V_\alpha$  is the water volume of compartment  $\alpha$  [m<sup>3</sup>],  $q_j$  and  $q_k$  are the volumetric flow rates [m<sup>3</sup>/s] of the  $j$ -th and  $k$ -th streams of fluid entering or exiting the compartment, respectively. There are  $J$  total streams entering compartment  $\alpha$  and  $K$  total streams exiting it. The left side of Equation (1) represents the instantaneous rate of change of compartment volume. Flow rates on the right side of Equation (1) are functions of time, geometry, salinity, and the physical properties governing water transport via evaporation and osmotic flow.

Likewise, mass conservation for salt within each compartment is

$$\frac{d(c_\alpha V_\alpha)}{dt} = \sum_j^J (c_j q_j)_{in} - \sum_k^K (c_k q_k)_{out} \quad (2)$$

where  $c_\alpha$ ,  $c_j$ , and  $c_k$  are the concentrations [mol/m<sup>3</sup>] of salt in compartment  $\alpha$ , in the  $j$ -th inlet stream, and in the  $k$ -th outlet stream, respectively. We consider tear salts as a single 1:1 aqueous electrolyte (i.e. NaCl). Therefore, concentrations reported as  $C$

below in osmolarity units refer to twice the molar concentration,  $2c$ .

Solution of coupled Equations (1) and (2) for compartment  $\alpha$  subject to the appropriate initial conditions gives the transient compartment volume and salinity,  $V_\alpha(t)$  and  $c_\alpha(t)$ , during each of the blink stages. We now outline the relevant physical processes for each compartment during each blink phase. Detailed equations are relegated to Appendix B of Supplementary Material.

### Deposition Phase

During the deposition stage of a blink, the upper lid rises to its open position.<sup>46</sup> As Wong et al.<sup>37</sup> describe, the upper meniscus deposits tear fluid onto the cornea and conjunctiva as the lid passes over the palpebral aperture. Outflow of fluid from the upper meniscus becomes the tear film. Thus, the upper meniscus coats the anterior corneal and conjunctival surfaces with a film of tear. The volume initially held in the upper meniscus alone is insufficient to provide fluid for a 3 to 5- $\mu\text{m}$  tear film and to retain a typical meniscus volume.<sup>47–49</sup> To account for this discrepancy, we postulate that a thin layer of tear from the conjunctival sac is uncovered from behind the upper-lid margin during lid upward motion. A hydrodynamic-lubrication analysis for the liquid between the corneal and lid-margin surfaces predicts the thin layer of tear between the two to be on the order of microns thick.<sup>50</sup> Accordingly, we select a 2- $\mu\text{m}$  gap between the lid wiper and the cornea. Fluid inflow into the upper meniscus prevents significant volume reduction as it leaves behind the tear film. Hydrodynamic coating theory quantifies the dependence of deposited tear-film thickness on upper meniscus radius  $R_{umr}$ , upper-lid velocity  $U$ , tear viscosity  $\mu$ , and tear surface tension  $\sigma$  (Equation B.4).<sup>37</sup> Equation (B.5) describes water conservation in the upper meniscus during deposition and, thus, deposited tear-film thickness. For the typical parameters listed in Table 1, a normal upper-meniscus radius of 300  $\mu\text{m}$  results in a 4- $\mu\text{m}$  thick deposited tear film in good agreement with current interferometric measurement.<sup>47</sup>

### Interblink Phase

Interblink is the 5-s phase between the end of deposition and the beginning of lid closure.<sup>46,51</sup> Fluid transfer via lacrimal secretion, corneal and conjunctival osmosis, punctal drainage, and tear evaporation occurs primarily during this longest period of the blink cycle.

**Conjunctival Sacs.** Both the upper and lower conjunctival sacs are approximated as rectangular channels of height  $h_c$  and lengths  $L_{uc}$  and  $L_{lc}$ , respectively, that span the width of the lids. For convenience, channel length is the areal-average distance from the

meniscus to the termination of the fornix. Freshly secreted tear flowing into the conjunctival sacs from the lacrimal glands with salt concentration  $c_{lac}$  is supplemented by osmotically driven water flow through the bulbar and palpebral conjunctivae wherever the salt concentration in the fornices is greater than that of the serum, approximated here as  $c_{lac}$ . Salt transport through epithelial cells is taken as negligible.<sup>41</sup> Conjunctival sacs serve as fixed-height conduits for tear fluid. Transient flow and solute concentration in the fornices are described by Equations (B.9) and (B.10), respectively.

**Menisci.** During interblink, tear fluid exiting the conjunctival sacs carries water and salt into each meniscus at the lid margins. Simultaneously, tears drain from the meniscus via suction through the puncta, and water evaporates from the exposed surface. Equations (B.11) and (B.13) describe water and salt mass conservation, respectively, in each meniscus. Drainage rate through the puncta is based on capillary suction, as previously enunciated by Zhu and Chauhan.<sup>23</sup> Thus, the drainage rate from the meniscus,  $q_{dir}$ , is proportional to the difference in curvatures between that of the meniscus, and that characteristic of the corresponding punctum, as quantified in Equation (B.12). That is, the larger is the meniscus radius of curvature,  $R_{imr}$ , the smaller is the opposing suction pressure in the meniscus and, therefore, the larger is the drainage rate. As a meniscus drains during an interblink, the meniscus radius of curvature decreases and the drainage rate subsides, and vice versa.<sup>38,51</sup> We account for evaporative loss of water from the menisci, but this loss is small compared to those in other compartments because of minimal exposed surface area.

**Tear Film.** At the beginning of interblink, suction from the upper and lower menisci rapidly pinches off the tear film to produce superior and inferior black lines.<sup>32,37,52,53</sup> The now-perched tear film is isolated from the menisci; flow between the menisci and the tear film is negligible.<sup>33</sup> During interblink, the tear film loses water to the environment by evaporation and gains water from osmotic imbibition through the cornea and conjunctiva, as described by Equation (B.14). We assume that the tear film resists dewetting for the entire interblink and ignore the presence of possible growing dimples and salinity hot spots in the tear film<sup>54–56</sup> or black lines.<sup>57</sup> Negligible salt transport occurs through the anterior corneal or conjunctival epithelium.<sup>41</sup> Therefore, salt initially present in the tear film concentrates according to Equation (B.15) as water evaporates into the environment. Evaporative tear loss is the physical origin of hyperosmolarity: evaporation concentrates salt in the tear film, which then distributes into the remaining tears during blinking. There can be no dry eye without tear evaporation.



### Closure Phase

At the end of interblink, the upper lid closes to meet the stationary lower lid. The lid meeting signifies the beginning of closure. During closure, motion of the lids and eyeball mixes the tear in the menisci with that in the tear film and, to a certain extent, with that in the upper and lower conjunctival sacs. We include a parameter,  $\beta_i$ , described in Appendix B, to characterize the extent of mixing in the upper and lower conjunctival sacs during closure,  $\beta_u$  and  $\beta_l$ .  $\beta_i$  ranges between 0 and 1, indicating no mixing and complete mixing. We find a minor effect of  $\beta$  on predicted tear osmolarity. Accordingly, we set  $\beta = 1$ , as stated earlier, because tear is assumed well mixed over many blinks. Consequently, upon completion of closure, the tear fluid exhibits a homogeneous bulk salt concentration,  $c_b$ , in the menisci, tear film, and conjunctival sacs. The bulk salt concentration  $c_b$ , calculated in Equation (B.16), is a volume-average salt concentration depending on the volumes and osmolarities in each compartment at the end of interblink. Capital symbol  $C_b = (2c_b)$  corresponds to measured tear osmolarity. After closure, deposition begins again starting with uniform salt concentration,  $c_b$ . During the course of deposition and interblink, compartment volumes redistribute and the osmolarities in each compartment change until they reset during the closure phase.

### Solution Methodology

Tear on the ocular surface is in a periodic-steady state. Otherwise, the tear thickness, menisci volumes, and salt concentrations drift in time to a new periodically repeated value. Therefore, the volumes and concentrations in each compartment must be the same at the beginning and end of each blink cycle. To conserve water in the periodic-steady state, the total amount of water flowing in and out of all five tear compartments over the three blink phases must be equal. As described in Appendix C of Supplementary Material, the total flow rate from the lacrimal and accessory lacrimal glands,  $q_{lac}$ , plus the total average flow rate of water through the cornea and conjunctiva,  $q_{cT}$ , must equal the average flow rate of tears into both puncta,  $q_d$ , plus the flow rate of water by evaporation from the tear film and menisci,  $q_e$ .

Conservation of salt in the periodic-steady state demands that the amount of salt supplied by the lacrimal and accessory lacrimal glands must equal that exiting in the tear draining through the puncta (Equation C.2). Upon imposition of periodicity, we utilize an iterative method to solve for the total tear volume,  $V_T$ , and volume-averaged bulk salt concentration,  $c_b$ . Specifically, after choosing an initial guess for the bulk salt concentration,  $c_b$ , and for the upper- and lower-meniscus radii of curvature at the beginning of deposition,  $R_b$ , we numerically integrate the

ordinary differential equations corresponding to the deposition, interblink, and closure balances by a Runge–Kutta algorithm, as outlined in Appendix C. An extended *Regula-Falsi* method<sup>58</sup> iterates on choices of  $c_b$  and  $R_b$  until the water and salt balances close over a complete blink cycle. Compared to a full transient solution,<sup>31</sup> computations are efficient because only the periodic-steady state need be ascertained.

### Parameters

#### Lacrimal Supply

Direct measurements of the lacrimal-supply rate,  $q_{lac}$ , in humans are not available. Instead, measurement of the TTR [%/min], permits calculation of  $q_{lac}$  using a model for tear flow over the ocular surface. There is a wealth of clinically measured TTRs in the literature, most of which are summarized in two recent reviews by Tomlinson et al.<sup>43,44</sup> TTR is determined quantitatively using fluorophotometry to gauge *in-situ* decay of a fluorescent dye instilled in the tears, neglecting any dye penetration into the cornea or conjunctiva. Typically, fluorescence in the tear film decays exponentially in time. The slope of the long-time portion of the log of fluorescent intensity versus time yields TTR.<sup>43–45</sup> Next, initial dye dilution allows calculation of the total tear volume,  $V_t$ . Calculation of  $q_{lac}$  from TTR and  $V_t$  is described in the literature<sup>27,43–45</sup> and in Appendix D of Supplementary Material. Current literature, however, ignores the contributions of osmotic imbibition and evaporation to tear flow. Although this is an accurate approximation for most healthy subjects, both of these flows are elevated for dry-eye patients.

To account for all flows in healthy and dry-eye patients (Equations D.2 and D.3), we require additional clinical measurement of the evaporative loss,  $q_e$ , and the bulk tear salinity,  $c_b$ . To our knowledge, two studies by Khanal et al.<sup>12,59</sup> provide the only data encompassing all necessary tear parameters to complete a rigorous analysis. Since lacrimal-supply rates of Khanal et al. are higher than average, we base our normal tear-supply value,  $1.10 \mu\text{L}/\text{min}$ , on the average tear flow established in the meta-analysis of Tomlinson et al.<sup>11,44</sup> We then use the data from Khanal et al.<sup>12,59</sup> to establish the ratios between lacrimal-supply and tear-evaporation rates in the normal and dry-eye cases. Tear supply is varied over a wide range to examine its effect on tear dynamics, especially on meniscus osmolarity. Representative healthy, dry-eye, ADDE, and EDE tear-supply rates are listed in Table 2.

#### Evaporation

Similar to the tear-flow data, *in-vivo* tear-evaporation rates have been reported for many decades and are summarized by Tomlinson et al.<sup>43,44</sup> Tear-evaporation

TABLE 2 Tear-evaporation and lacrimal-supply rates for normal and dry eyes.

| Case                             | Tear-evaporation rate, $q_e$ [ $\mu\text{L}/\text{min}$ ] | Lacrimal-supply rate, $q_{lac}$ [ $\mu\text{L}/\text{min}$ ] |
|----------------------------------|---|--|
| Normal                           | 0.15  | 1.10   |
| Dry eye                          | 0.30  | 0.55   |
| Aqueous-deficient dry eye (ADDE) | 0.25  | 0.40   |
| Evaporative dry eye (EDE)        | 0.35  | 0.80   |

measurements on the human eye generally come in two forms. The most common measurement involves placing specially designed goggles over the eye to measure water loss from the ocular surface.<sup>43,44,60–64</sup> The second method employs optical interferometry to measure the tear-film thinning rate at a specific spot in the tear film.<sup>36</sup> Evaporation rates measured with interferometry are significantly higher than those obtained with goggle wear.<sup>43</sup> We chose the average reported evaporation rate from the meta-analysis of Tomlinson et al.,<sup>43</sup>  $0.75 \mu\text{m}/\text{min}$  ( $0.15 \mu\text{L}/\text{min}$ ), for normals. In choosing the tear-evaporation rates for various dry-eye scenarios, we again use the ratios of evaporation rates provided by Khanal et al.<sup>12,59</sup>

Separately, we study high evaporation rates measured interferometrically by Nichols et al.<sup>36</sup> and fluorescently by King-Smith et al.<sup>35</sup> Nichols et al.<sup>36</sup> measured an average thinning rate of  $3.79 \mu\text{m}/\text{min}$  in a  $33 \times 35 \mu\text{m}$  patch of the precorneal tear film. Using fluorescence imaging, King-Smith et al.<sup>35</sup> estimated evaporation rates in precorneal and preconjunctival tear films to be  $2.4$  and  $1.4 \mu\text{m}/\text{min}$ , respectively. We approximate the overall evaporation rate to be the average of the two rates, or  $1.9 \mu\text{m}/\text{min}$ . By considering these evaporation rates, we investigate how high the tear-supply rate or osmotic water permeability of the cornea and conjunctiva must be to produce normal bulk tear osmolarity.

### Tissue Water Permeability

In contrast to the above tear parameters, all estimated from measurements on humans, whole-tissue water permeability has been directly measured only on animals.<sup>22</sup> Mouse eyes yielded corneal and conjunctival-tissue water permeabilities of  $1.7$  and  $1.1 \times 10^{-5}$  m/s, respectively. Recently reported measurements of evaporation and fluorescence decay in human eyes<sup>35</sup> indirectly estimate these permeabilities to be about  $1.2$  and  $5.5 \times 10^{-5}$  m/s, respectively. Mathematical modeling of corneal metabolism and water transport<sup>41</sup> also gives a corneal water permeability of  $2.1 \times 10^{-5}$  m/s, with a basal transcorneal secretion rate of  $0.013 \mu\text{L}/\text{min}$ .<sup>42</sup> In this work, the value  $1.25 \times 10^{-5}$  m/s was chosen for both corneal and conjunctival water permeability. We also adopt the basal water-secretion rate from Leung et al.,<sup>41</sup> which is not a

function of osmolarity. These values agree with the small body of available literature,<sup>22,35,41</sup> and result in tear osmolarities that match reported values for normal and dry eyes.<sup>11</sup> Since altering tissue water permeabilities results in significant changes in predicted tear dynamics, we also investigate the effect of varying them as parameters.

## RESULTS

### Normal and Dry-Eye Conditions

Given the parameters in Table 1 for normal individuals, the coupled water and salt balances predict the periodic-steady-state tear dynamics. Additionally, we predict behavior for tear-evaporation and lacrimal-supply rates representative of all dry eye (DE), ADDE, and EDE, as listed in Table 2. Figures 3 and 4 show the periodic-steady osmolarities and volumes of various compartments over five blink cycles for normal and dry-eye conditions. Right brackets in each figure differentiate between normal and dry-eye subjects. Solid, dotted, and dashed lines in Figure 3 correspond to the tear-film, menisci, and conjunctival-sac osmolarities, respectively. Osmolarity differences between the upper and lower menisci and conjunctival sacs are negligible. Solid, dotted, and dashed lines in Figure 4 correspond to the tear-film, upper-meniscus, and lower-meniscus tear volumes, respectively. Also shown is the deposition time-averaged tear-film thickness,  $\langle h_{if} \rangle$ . The total volume of the conjunctival sacs is constant at  $4.5 \mu\text{L}$  for all cases, or  $2.25 \mu\text{L}$  each. Just after tear deposition to the left of a cycle, each compartment begins with an initial volume and osmolarity. During 5-s interblink, fluid and solute obey the conservation balances, causing gradual changes in compartment osmolarity and volume. At the end of interblink to the right of a blink cycle, closure occurs, mixing the compartments and resetting their volumes and salinities back to their initial states before deposition. Clearly, the tear-film osmolarity increases during the interblink because water evaporation exceeds osmotic inflow. Osmotic imbibition causes the small decline in the fornix osmolarity during interblink. Figure 3 shows minimal changes in meniscus osmolarity during the blink cycle. Therefore, the bulk-tear osmolarity,  $C_b$ , is representative of that in the lower meniscus, from which clinical samples are obtained.<sup>6,8,9,11</sup> Water evaporation from the tear film demands that the bulk-tear osmolarity always be greater than that of the isotonic secreted lacrimal tears.

For normal conditions, the upper meniscus begins interblink with 40% less volume than that in the lower meniscus. This is because the upper meniscus supplies the tear-film volume. Since the majority of the lacrimal tear supply arrives from the upper fornix, the upper meniscus grows by 6% in volume

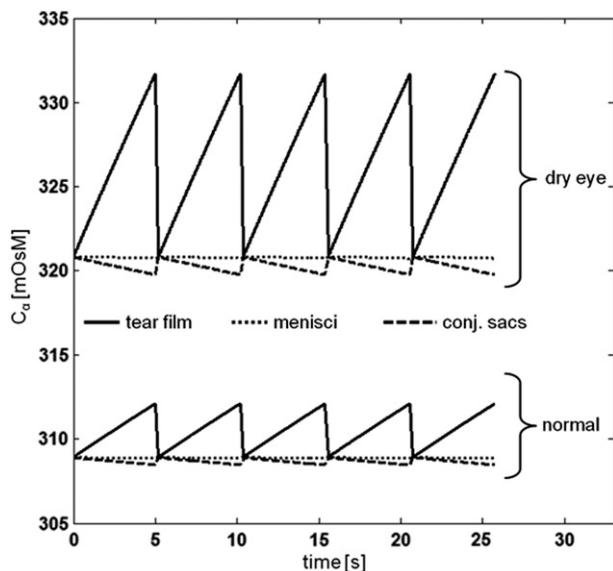


FIGURE 3 Periodic-steady-state osmolarities of upper and lower meniscus, conjunctival sacs, and tear film over five blink cycles for normal and dry-eye conditions. Solid, dotted, and dashed lines correspond to the tear film, the menisci, and the conjunctival sacs, respectively. The osmolarity difference between the upper and lower conjunctival sacs and menisci is negligible. Brackets indicate normal ( $q_e = 0.15 \mu\text{L}/\text{min}$ ;  $q_{lac} = 1.10 \mu\text{L}/\text{min}$ ) and dry-eye conditions ( $q_e = 0.30 \mu\text{L}/\text{min}$ ;  $q_{lac} = 0.55 \mu\text{L}/\text{min}$ ).

during interblink whereas the lower meniscus drains more than it gains, shrinking by 3% in volume. Menisci volumes at the commencement of deposition are identical, corresponding to the curvature radius  $R_b$ . For clarity of viewing, the instantaneous volume spike for the upper meniscus is not shown in Figure 4. Rather, upper-meniscus menisci volumes at the commencement of closure and the end of deposition are connected by straight lines. During tear-film deposition, the upper-meniscus volume corresponding to  $R_b$  shrinks rapidly to its initial interblink value.

The tear film loses about 1% of its volume and thickness to evaporation during interblink. Thus, the tear film, which is initially at 309 mOsM, experiences a 3-mOsM spike due to evaporation. Conversely, upper and lower conjunctival sacs receive fresh tear from the lacrimal glands and water through the conjunctiva, slightly diluting their osmolarities. Also, menisci receive fresh tears from the conjunctival sacs, which outweighs the minor concentrating effect of evaporation.

Overall, the situation is similar for dry-eye conditions, as illustrated in Figures 3 and 4. Changes in lacrimal supply and evaporation rates, however, cause quantitative differences. As shown in Table 2, we use 0.55 and  $0.30 \mu\text{L}/\text{min}$  for lacrimal-secretion and tear-evaporation rate in dry eye, respectively. A decreased lacrimal supply shrinks the dry-eye upper and lower menisci volumes to less than one-half

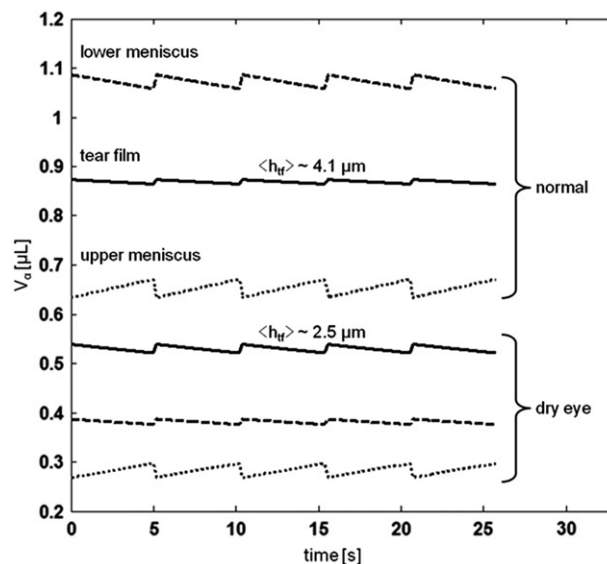


FIGURE 4 Periodic steady-state volumes of upper and lower meniscus and tear film over five blink cycles for normal and dry-eye conditions. Solid, dotted, and dashed lines correspond to the tear film, the upper meniscus, and the lower meniscus, respectively. The total volume of the conjunctival sacs is constant at  $4.5 \mu\text{L}$  for all cases. Right brackets indicate normal ( $q_e = 0.15 \mu\text{L}/\text{min}$ ;  $q_{lac} = 1.10 \mu\text{L}/\text{min}$ ) and dry-eye conditions ( $q_e = 0.30 \mu\text{L}/\text{min}$ ;  $q_{lac} = 0.30 \mu\text{L}/\text{min}$ ). The deposition time-averaged tear-film thickness is labeled as 4.1 and  $2.5 \mu\text{m}$  for normal and dry-eye subjects, respectively.

(43 and 36%) of their normal values, while the tear-film volume and thickness decreases to 62% of their normal values. Increased tear-evaporation and decreased lacrimal-supply rates elevate  $C_b$  to 321 mOsM, 12 mOsM greater than that under normal conditions. Increased evaporation causes the tear-film osmolarity to spike strongly during interblink to 11 mOsM above the bulk osmolarity. Most importantly, the epithelial cells of the cornea and exposed conjunctiva experience the spikes in osmolarity, whereas the measured osmolarity of the menisci,  $C_b$ , remains lower and essentially constant.

### Tear-Evaporation and Lacrimal Secretion

By varying tear-evaporation and lacrimal-supply rates while holding all other parameters constant, we explore a wide range of possible tear-dynamics scenarios. Figures 5 and 6 show contour plots of bulk tear osmolarity,  $C_b$ , and of total transcorneal and transconjunctival water flow,  $q_{cT}$ , as a function of evaporation rate  $q_e$  and lacrimal-supply rate  $q_{lac}$ . Contour lines for  $C_b$  in Figure 5 appear every 5 mOsM between 305 and 335 mOsM, and those for  $q_{cT}$  in Figure 6 appear every  $0.05 \mu\text{L}/\text{min}$  between 0.05 and  $0.45 \mu\text{L}/\text{min}$ . For reference, open markers are placed on the graphs at the locations representing normal ( $\circ$ ), dry-eye ( $\square$ ), ADDE ( $\nabla$ ), and EDE ( $\triangle$ ) conditions. Reported osmolarities correspond to those

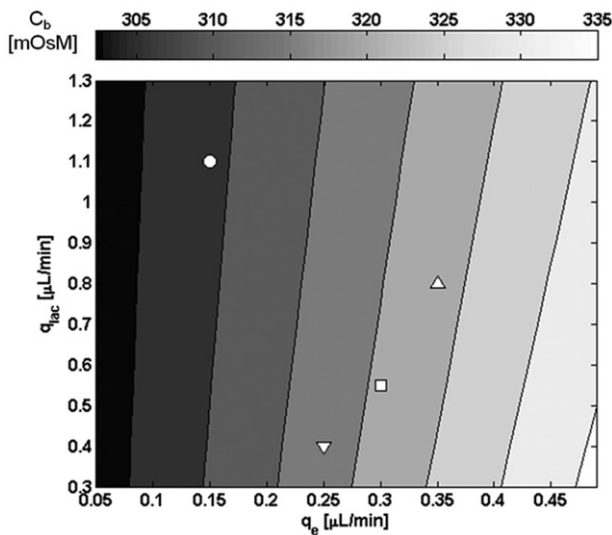


FIGURE 5 Contours of bulk tear osmolarity,  $C_b$ , as a function of tear-evaporation rate,  $q_e$ , and lacrimal-supply rate,  $q_{lac}$ . Contour lines for  $C_b$  appear every 5 mOsM between 305 and 335 mOsM. Open markers signify normal (○), dry-eye (□), ADDE (▽), and EDE (△) conditions as described in Table 2. Predicted osmolarities for normal, dry-eye, ADDE, and EDE conditions are 309, 321, 317, and 323 mOsM, respectively.

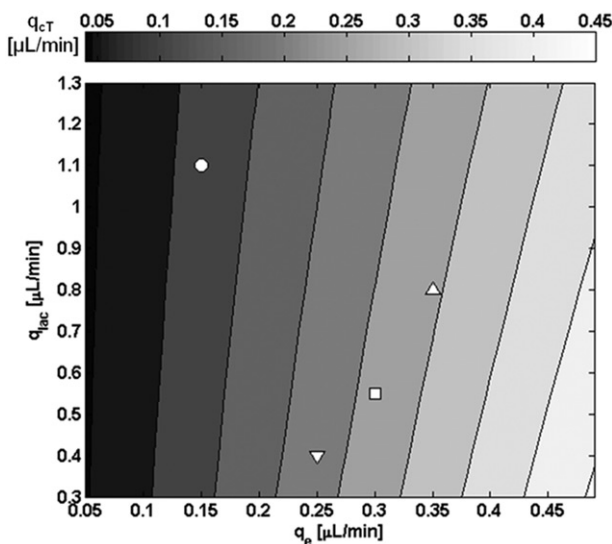


FIGURE 6 Contours of total transcorneal and transconjunctival water flow,  $q_{cT}$ , as a function of tear-evaporation rate,  $q_e$ , and lacrimal-supply rate,  $q_{lac}$ . Contour lines for  $q_{cT}$  appear every 0.05  $\mu\text{L}/\text{min}$  between 0.05 and 0.45  $\mu\text{L}/\text{min}$ . Open markers signify normal (○), dry-eye (□), ADDE (▽), and EDE (△) conditions as described in Table 2. Predicted total transmembrane water flows for normal, dry-eye, ADDE, and EDE conditions are 0.12, 0.26, 0.23, and 0.29  $\mu\text{L}/\text{min}$ , respectively.

in the lower meniscus not those actually experienced by the corneal epithelium.

As expected, tear osmolarity increases as evaporation rate increases and lacrimal supply decreases. Osmolarities predicted by our model for normal, dry-eye, ADDE, and EDE conditions are 309, 321, 317, and

323 mOsM, respectively. Data in Figure 6 demonstrate that increasing tear evaporation and decreasing lacrimal supply increases the osmotic water inflow  $q_{cT}$  because higher salinity increases osmotic water withdrawal through the cornea and conjunctiva. Total osmotic water flows predicted by our model for normal, dry-eye, ADDE, and EDE conditions are 0.12, 0.26, 0.23, and 0.29  $\mu\text{L}/\text{min}$ , respectively.

Appendix E of the Supplementary Material contains predictions for additional clinically relevant tear-dynamics as functions of tear-evaporation and lacrimal-supply rates. Figures E1–E5 show predictions of TTR, average deposited tear-film thickness, maximum tear-film osmolarity, initial meniscus radius during deposition, and total tear volume, respectively, for the same range of  $q_e$  and  $q_{lac}$  as those in Figures 5 and 6. TTR are predicted at 14.7, 8.6, 6.5, and 11.7%/min for normal, dry-eye, ADDE, and EDE conditions (Figure E1). Corresponding clinically measured values are 15.2, 7.8, 5.7, and 12.6%/min for the same cases.<sup>12,59</sup> Although there is only a 2% difference in  $C_b$  between ADDE and EDE, the TTR in EDE is 80% higher than that in ADDE. The increased TTR in EDE results from a much higher tear-supply rate in EDE compared to that in ADDE despite similar total tear volumes in both conditions.

With the highest evaporation rates measured by King-Smith et al.<sup>35</sup> and Nichols et al.,<sup>36</sup> of 0.40 and 0.76  $\mu\text{L}/\text{min}$ , and normal lacrimal-supply rate, corneal and conjunctival water permeability values, the blink model predicts  $C_b$  of 335 mOsM and 370 mOsM, respectively. We investigate how much  $q_{lac}$  or  $P_{cj}$  and  $P_{cn}$  must increase to predict a normal salt osmolarity of 309 mOsM. For simplicity, we set  $P_{cj} = P_{cn}$ . With evaporation rates of 0.40 and 0.76  $\mu\text{L}/\text{min}$  and a fixed  $P_{cn} = P_{cj}$  of  $1.25 \times 10^{-5}$  m/s,  $q_{lac}$  must increase from 1.10 to 11 and 22  $\mu\text{L}/\text{min}$ , respectively, or more than tenfold. Lacrimal-supply rates this far outside the normal range necessitate increasing the maximum drainage rate to enable sufficient drainage to prevent tear overflow. For  $q_{lac}$  fixed at 1.10  $\mu\text{L}/\text{min}$  with the same evaporation rates, then  $P_{cn}$  and  $P_{cj}$  must increase to  $11.5 \times 10^{-5}$  and  $6.3 \times 10^{-5}$  m/s, respectively. To mimic dry eye under these conditions, we doubled  $q_e$  and halved  $q_{lac}$ . With fixed  $P_{cn}$  and  $P_{cj}$  and increased  $q_{lac}$ , predicted  $C_b$  increases to  $\sim 330$  mOsM at both evaporation rates. With fixed  $q_{lac}$  and increased  $P_{cn}$  and  $P_{cj}$ ,  $C_b$  increases from 309 to  $\sim 315$  mOsM at both evaporation rates.

### Conjunctival and Corneal Water Permeability

The water permeability of the cornea and the conjunctiva to osmotic flow are varied independently from  $5 \times 10^{-7}$  to  $4 \times 10^{-5}$  m/s while fixing the evaporation and lacrimal-supply rates constant.



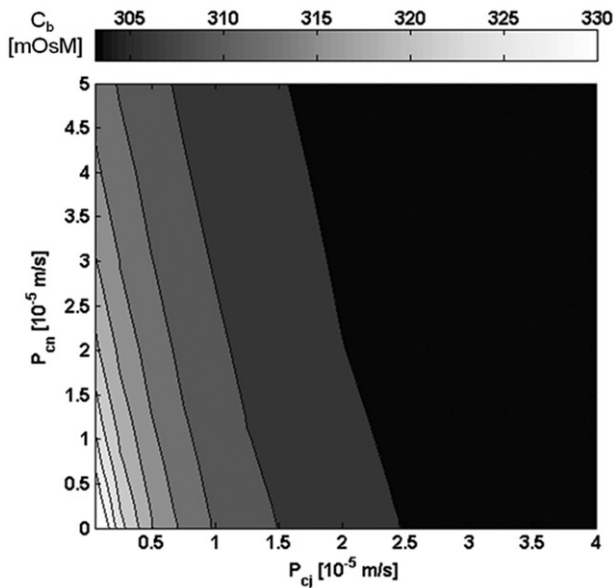


FIGURE 7 Contours of bulk tear osmolarity,  $C_b$ , reported as osmolarity, as a function of conjunctival,  $P_{cj}$ , and corneal permeability,  $P_{cn}$  for normal conditions ( $q_{lac} = 1.10 \mu\text{L}/\text{min}$ ;  $q_e = 0.15 \mu\text{L}/\text{min}$ ). Contour lines appear every 3 mOsM between 306 and 330 mOsM. Normal permeability in this model is  $P_{cj} = P_{cn} = 1.25 \times 10^{-5} \text{ m/s}$  corresponding to  $C_b = 309 \text{ mOsM}$ . At  $P_{cj} = P_{cn} = 0$ ,  $C_b = 344 \text{ mOsM}$ .

Changes in water permeability affect the dynamics of all tear compartments, but the most important metric is tear osmolarity. Figure 7 shows the contours of bulk tear osmolarity,  $C_b$ , over the range of  $P_{cn}$  and  $P_{cj}$  for normal lacrimal-supply and tear-evaporation rates. Contour lines in Figure 7 appear every 3 mOsM between 306 and 330 mOsM. Osmolarity decreases as both permeabilities increase. Due to the large surface area of the conjunctiva, conjunctival permeability plays a stronger role in determining meniscus osmolarity than does the corneal permeability. As both  $P_{cn}$  and  $P_{cj}$  approach zero, tear osmolarity under normal lacrimal-supply and evaporation conditions increases rapidly towards that observed in dry eye. In the limit of zero transcorneal or transconjunctival osmotic flow,  $C_b$  equals 344 mOsM.

## DISCUSSION

The proposed periodic-steady tear-dynamics model includes realistic description of tear drainage, tear-film deposition, and under-lid flow to capture actual tear-system physics. Periodic-steady state is reasonable because blinking occurs frequently compared to the changes in environmental conditions that set tear-evaporation and lacrimal-supply rates. Notable exceptions follow application of topical eye-care solutions, in which case time is required for the tear volume and

osmolarity to reset to their normal, periodic-steady values.

The tear-dynamics model demonstrates the importance of osmotic-driven water flow through the cornea and conjunctiva. Under normal conditions, we predict a meniscus osmolarity of 309 mOsM, slightly higher than the average of all reported tear osmolarities, 302 mOsM,<sup>11,12,65</sup> but close to the 308 mOsM value reported by Khanal et al.<sup>12,59</sup> Because water flow through the ocular surface counteracts the concentrating effect of evaporation, our tear dynamics matches the observed osmolarity without limitation to low evaporation rates and high lacrimal supply rates.<sup>31</sup> Without osmotic imbibition, tear osmolarity under normal conditions reaches 344 mOsM, well above that measured in healthy individuals.<sup>6,8,9,11,12,59,65</sup> In our calculations, osmotic-driven water flow accounts for 10% of the total water supply under normal conditions. This amount is less than the 25% predicted by Zhu and Chauhan,<sup>26</sup> who use an evaporation rate that is over 5 times higher than the average reported tear-evaporation rate and an extremely high secreted-tear osmolarity (necessitating greater water secretion to prevent hyperosmolarity). In dry eye, increased tear osmolarity drives the osmotic water flow up to 0.26  $\mu\text{L}/\text{min}$ , or almost 50% of the lacrimal-supply rate, making it a significant contributor to tear flow. Thus, analysis of fluorescent-dyed tear-flow experiments must account for this diluting effect. The magnitudes of osmotic water flow into the upper conjunctival sac, lower conjunctival sac, and tear film are approximately equal under healthy conditions. In dry eye, however, evaporation-driven hyperosmolarity in the tear film intensifies, causing the relative contribution of osmotically driven flow into the tear film to increase.

By varying the lacrimal-supply and tear-evaporation rates, in Figures 5 and 6 and Figures E1-E5, we investigate the effect of dry-eye conditions on tear dynamics. Increasing evaporation and decreasing lacrimal supply generally decreases TTR, total tear volume, meniscus radii, and tear-film thickness while increasing osmolarity and transcorneal/conjunctival water flow. Figure E1 indicates that TTR is an exception when  $q_{lac}$  is above 1.2–1.3  $\mu\text{L}/\text{min}$ . These trends are in agreement with clinical data<sup>11,59,66,67</sup> and with previous modeling efforts.<sup>26,31</sup> Although, in general, tear osmolarity increases for dry eye, EDE exhibits the highest osmolarity and ADDE the lowest. The difference, though, is only 5 mOsM, or less than 2%, which makes it a poor clinical discriminator between the two dry-eye subcases. Higher osmolarity with EDE suggests that it causes the most hyperosmotic damage and is a more severe form of dry eye. Total tear volume, meniscus radii, and tear-film thickness all increase with increasing lacrimal supply rate. There are modest differences in these variables between ADDE and EDE, but TTR is the



single best differentiator. TTR in EDE is 12%/min, which is double the value for ADDE, 6%/min. This result compares closely with those of Khanal et al.,<sup>12,59</sup> who report TTRs of 13 and 6%/min for EDE and ADDE, respectively. We corroborate the conclusion of Khanal et al.<sup>59</sup> that tear osmolarity is a useful clinical indicator of dry eye in general, and that TTR can be used to discriminate between the ADDE and EDE subtypes.

We predict tear osmolarities of 335 and 370 mOsm for the higher evaporation rates reported by King-Smith et al.<sup>35</sup> and Nichols et al.,<sup>36</sup> respectively, with otherwise normal physical parameters. These osmolarities are clearly too high for a healthy subject. To predict normal osmolarities at these evaporation rates,  $q_{lac}$  or  $P_{cn}$  and  $P_{cj}$  must increase significantly. All else being equal,  $q_{lac}$  must be 10–20 times the average reported value of 1.10  $\mu\text{L}/\text{min}$ . Even the highest clinical measurements are not close to this value.<sup>27,68</sup> Alternatively, osmotic imbibition through the cornea and conjunctiva could provide the extra water to offset hyperosmolarity induced by the increased evaporation. For evaporation rates of 0.40 and 0.76  $\mu\text{L}/\text{min}$ , increasing  $P_{cn}$  and  $P_{cj}$  to 6.25 or  $11.5 \times 10^{-5}$  m/s, respectively, enables enough water flow through the ocular surface to generate a normal tear osmolarity. Although these values are about 5–10 times higher than the values adopted for a healthy eye, lack of human data makes it difficult to ascertain whether these values are unrealistic. Such high tissue-water permeabilities, however, result in inconsistencies between the model and observations. When already high evaporation rates are doubled and the tear supply is halved to simulate dry-eye conditions, the bulk-average tear osmolarity rises to about 315 mOsm, which is only 6 mOsm higher than the healthy case. Thus, with high water permeabilities, increased evaporation and decreased lacrimal supply do not lead to significant hyperosmolarity as observed clinically.

These findings suggest that the average tear-evaporation rate over the entire exposed tear surface must be lower than the localized measurements of 1.9–3.79  $\mu\text{m}/\text{min}$  by King-Smith et al.<sup>35</sup> and Nichols et al.<sup>36</sup> As King-Smith et al. report,<sup>35</sup> the tear-evaporation rate varies across the eye, probably due to local differences in lipid-layer thickness and airflow. We expect that the lipid layer is thickest near its origin at the meibomian glands and the airflow is also the lowest in these regions compared to those in the middle of the palpebral aperture. Thus, the evaporation rate should be highest in the middle, where both Nichols et al.<sup>36</sup> and King-Smith et al.<sup>35</sup> measure thinning rates. In contrast, goggle experiments, which detect total water loss from the ocular surface, establish an average evaporation rate over the entire exposed tear film. Additional experiments are necessary to reconcile the goggle and open-environment evaporation measurements.

Results in Figure 7 not only show the significant effect of corneal/conjunctival water permeability but also give upper and lower bounds to these values. Although larger permeabilities yield lower tear osmolarities, permeabilities that are too high effectively render the ocular surface so water permeable that hyperosmolarity cannot occur even under dry-eye conditions. At the other extreme, lower permeabilities produce very high osmolarities for dry-eye and normal conditions alike. Given that most osmotically driven water transport is transcellular and that the corneal epithelium contains more tight junctions than does the conjunctival epithelium, it seems reasonable to assume that the conjunctival water permeability should not be less than that of the cornea. Experimental data support<sup>35</sup> and contest<sup>22</sup> this statement. Only a small range of tissue water permeabilities for our given set of evaporation and lacrimal-supply rates generates osmolarities in agreement with clinically measured values. This range of permeabilities lies near  $10^{-5}$  m/s, very close to all experimentally measured values and model predictions, and lends confidence to our tear-dynamics model. From the tissue water permeabilities of Leung et al.,<sup>41</sup> we find that the cornea plays a significant role in supplying water to the tear film. Previous models neglected this important contribution.<sup>26</sup>

There are several limitations to the proposed tear-dynamics model, due mainly to lack of quantitative parameters. An issue of particular concern is the choice of a “normal” evaporation rate. We chose average values from the meta-analysis by Tomlinson et al.<sup>43</sup> that covers 437 patients from 15 studies from about 10 different authors. Despite these extensive data, two main issues arise with tear-evaporation measurements. First, measured evaporation rates range over two orders of magnitude, from 0.02 to  $6.3 \times 10^{-6}$  g/cm<sup>2</sup>/s. Evaporation rates from different ends of this spectrum yield extremely different tear osmolarities. And, importantly, evaporation rate depends on airflow, environmental humidity, and temperature. There is no one tear-evaporation rate. Therefore, averaging over a large subject size is irrelevant if the airflow and ambient conditions are not controlled and representative.

Another limiting factor is the absence of experiments in which a sufficient number of tear variables is measured. Most experiments do not measure simultaneously TTR, tear volume, evaporation rate, and osmolarity. Unless all of these measurements are taken, lacrimal-tear supply and osmotically driven water flow cannot be disentangled. More experiments similar to those of Khanal et al.<sup>12,59</sup> are needed. To address this issue, we used average values from the larger body of literature, but applied the ratios of tear flow in ADDE or EDE conditions from those reported by Khanal et al.<sup>12,59</sup> Our model can be refined as more detailed tear-flow data become available.

Despite limitations, our proposed periodic-steady tear-dynamics model captures the basic physics of water and salt dynamics in the eye self-consistently and agrees well with available clinical data. One important application is topical delivery of drugs or care solutions to the ocular surface. The normal TTR is so high that instilled fluids and solutes are rapidly removed from the eye, minimizing drug availability. Maximizing the residence time of these substances on the eye is important to topical delivery of drugs and eye-care solutions. Although we focus on salt osmolarity here, the presented solute balances are general and readily extended to drugs, fluorescent tracers, or other solutes of interest. Studying the dynamics of instilled drugs can guide treatment regimens to maximize bioavailability of topically delivered drug molecules. Additionally, introduction of the viscosity dependence of the tear-drainage rate can predict the role of viscosity enhancers in lengthening residence time of either fluid or solute on the eye.

### ACKNOWLEDGEMENTS

The authors thank A. Tomlinson and M. C. Lin for valuable clinical insights during the formulation of this model, A. Chauhan for helpful discussion, and J. Newman for proposing the two-parameter *Regula Falsi* solution method. C.F.C. acknowledges Alcon Corporation for partial funding.

### DECLARATION OF INTEREST

This study was partially supported by Alcon under Contract 022466-003 to the University of California. The authors declare no conflicts of interests. The authors alone are responsible for the content and writing of this article.

### REFERENCES

- (No authors listed). The epidemiology of dry eye disease: report of the epidemiology subcommittee of the international dry eye workshop (2007). *Ocul Surf* 2007;5:93–107.
- (No authors listed). The definition and classification of dry eye disease: report of the definition and classification subcommittee of the international dry eye workshop (2007). *Ocul Surf* 2007;5:75–92.
- Von Bahr G. Konte der flüssigkeitsabgang durch die cornea von physiologischer bedeutung sein? *Acta Ophthalmol* 1941;19:125–134.
- Balik J. The lacrimal fluid in keratoconjunctivitis sicca: a quantitative and qualitative investigation. *Am J Ophthalmol* 1952;35:773–782.
- Mastman GJ, Baldes EJ, Henderson JW. The total osmotic pressure of tears in normal and various pathologic conditions. *Arch Ophthalmol* 1961;65:509–513.
- Gilbard JP, Farris RL, Santamaria J. Osmolarity of tear microvolumes in keratoconjunctivitis sicca. *Arch Ophthalmol* 1978;96:677–681.
- Gilbard JP, Farris RL. Tear osmolarity and ocular surface disease in keratoconjunctivitis sicca. *Arch Ophthalmol* 1979;97:1642–1646.
- Suzuki M, Massingale ML, Ye F, Godbold J, Elfassy T, Vallabhajosyula M, et al. Tear osmolarity as a biomarker for dry eye disease severity. *Invest Ophthalmol Vis Sci* 2010;51:4557–4561.
- Sullivan BD, Whitmer D, Nichols KK, Tomlinson A, Foulks GN, Geerling G, et al. An objective approach to dry eye severity. *Invest Ophthalmol Vis Sci* 2010;51:6125–6130.
- Farris RL. Tear osmolarity - a new gold standard? *Adv Exp Med Biol* 1994;350:495–503.
- Tomlinson A, Khanal S, Ramaesh K, Diaper CJM, McFayden A. Tear film osmolarity: determination of a referent for dry eye diagnosis. *Invest Ophthalmol Vis Sci* 2006;47:4309–4315.
- Khanal S, Tomlinson A, McFayden A, Diaper CJM, Ramaesh K. Dry eye diagnosis. *Invest Ophthalmol Vis Sci* 2008;49:1407–1414.
- Korb DR, Craig JP, Doughty M, Guillon J-P, Smith G, Tomlinson A. The tear film: structure, function, and clinical examination. Oxford: Butterworth-Heinemann; 2002.
- Bron AJ, Tiffany JM. The contribution of meibomian disease to dry eye. *Ocul Surf* 2004;2:149–164.
- Bron AJ, Tiffany JM, Gouveia SM, Yokoi N, Voon LW. Functional aspects of the tear film lipid layer. *Exp Eye Res* 2004;78:347–360.
- Foulks GN, Bron AJ. Meibomian gland dysfunction: a clinical scheme for description, diagnosis, classification, and grading. *Ocul Surf* 2003;1(3):107–126.
- Chen W, Zhang X, Zhang J, Chen J, Wang S, Wang Q, et al. A murine model of dry eye induced by an intelligently controlled environmental system. *Invest Ophthalmol Vis Sci* 2008;49:1386–1391.
- McCulley JP, Aronowicz JD, Uchiyama E, Shine WE, Butovich IA. Correlations in a change in aqueous tear evaporation with a change in relative humidity and the impact. *Am J Ophthalmol* 2006;141:758–760.
- Niedererkorn JY, Stern ME, Pflugfelder SC, De Paiva CS, Corrales RM, Gao J, et al. Desiccating stress induces t cell-mediated sjögren's syndrome-like lacrimal keratoconjunctivitis. *J Immunol* 2006;176:3950–3957.
- Bron AJ, Yokoi Y, Gaffney EA, Tiffany JM. Predicted phenotypes of dry eye: proposed consequences of its natural history. *Ocul Surf* 2009;7:78–92.
- Baudouin C. The pathology of dry eye. *Surv Ophthalmol* 2001;45:S211–S220.
- Levin MH, Verkman AS. Aquaporin-dependent water permeation at the mouse ocular surface: in vivo micro-fluorimetric measurements in cornea and conjunctiva. *Invest Ophthalmol Vis Sci* 2004;45:4423–4432.
- Zhu H, Chauhan A. A mathematical model for tear drainage through the canaliculi. *Curr Eye Res* 2005;30:621–630.
- Zhu H, Chauhan A. A mathematical model of tear mixing under the lower lid. *Curr Eye Res* 2007;32:1023–1035.
- Zhu H, Chauhan A. A mathematical model for ocular tear and solute balance. *Curr Eye Res* 2005;30:841–854.
- Zhu H, Chauhan A. Tear dynamics model. *Curr Eye Res* 2007;32:177–197.
- Mishima S, Gasset A, Klyce SD, Baum JL. Determination of tear volume and tear flow. *Invest Ophthalmol* 1966;5:264–276.

28. Port MJA, Asaria TS. The assessment of human tear volume. *Cont Lens Anterior Eye* 1990;13:76–82.
29. Fraunfelder FT. Extraocular fluid dynamics: how best to apply topical ocular medication. *Trans Am Ophthalmol Soc* 1976;74:457–487.
30. Macdonald EA, Maurice DM. The kinetics of tear fluid under the lower lid. *Exp Eye Res* 1991;53:421–425.
31. Gaffney EA, Tiffany JM, Yokoi N, Bron AJ. A mass and solute balance model for tear volume and osmolarity in the normal and dry eye. *Prog Retin Eye Res* 2010;29:59–78.
32. McDonald JE, Brubaker S. Meniscus-induced thinning of tear films. *Am J Ophthalmol* 1971;72:139–146.
33. Miller KL, Polse KA, Radke CJ. Black-line formation and the “perched” human tear film. *Curr Eye Res* 2002;25:155–162.
34. Bron AJ, Tiffany JM, Yokoi N, Gouveia SM. Using osmolarity to diagnose dry eye: a compartmental hypothesis and review of our assumptions. In: Sullivan DA, Stern ME, Tsubota K, Dartt DA, Sullivan RM, Bromberg BB, editors. *Lacrimal gland, tear film, and dry eye syndromes 3: basic science and clinical relevance, pts a & b; 2002*. New York: Springer, pp 1087–1095.
35. King-Smith PE, Ramamoorthy P, Nichols KK, Braun RJ, Nichols JJ. If tear evaporation is so high, why is osmolarity so low? In *The 6th International Conference on the Tear Film & Ocular Surface; 2010; Florence, ITA*.
36. Nichols JJ, Mitchell GJ, King-Smith PE. Thinning rate of the precorneal and prelens tear films. *Invest Ophthalmol Vis Sci* 2005;46:2353–2361.
37. Wong H, Fatt I, Radke CJ. Deposition and thinning of the human tear film. *J Colloid Interface Sci* 1996;184:44–51.
38. Maurice DM. The dynamics and drainage of tears. *Int Ophthalmol Clin* 1973;13:103–116.
39. Murube J. Tear osmolarity. *Ocul Surf* 2006;4:62–73.
40. Candia OA. Electrolyte and fluid transport across corneal, conjunctival and lens epithelia. *Exp Eye Res* 2004;78:527–535.
41. Leung BK, Bonanno JA, Radke CJ. A model for corneal metabolism. *Prog Retin Eye Res* 2011;30:471–492.
42. Cerretani C, Peng C-C, Chauhan A, Radke CJ. Aqueous salt transport through soft contact lenses: an osmotic-withdrawal mechanism for prevention of adherence. *Contact Lens Anterior Eye* 2012;35:260–265.
43. Tomlinson A, Doane MG, McFayden A. Inputs and outputs of the lacrimal system: review of production and evaporative loss. *Ocul Surf* 2009;7:186–198.
44. Tomlinson A, Khanal S. Assessment of tear film dynamics: quantification approach. *Ocul Surf* 2005;3:81–95.
45. Van Best JA, Benitez del Castillo JM, Coulangeon L-M. Measurement of basal tear turnover using a standardized protocol. *Graefes Arch Clin Exp Ophthalmol* 1995;233:1–7.
46. Doane MG. Interactions of eyelids and tears in corneal wetting and the dynamics of the normal human eyeblink. *Am J Ophthalmol* 1980;89:507–516.
47. King-Smith PE, Fink B, Hill R, Koelling K, Tiffany JM. The thickness of the tear film. *Curr Eye Res* 2004;29:357–368.
48. Jones MB, Please CP, McElwain DLS, Fulford GR, Roberts AP, Collins MJ. Dynamics of tear-film deposition and draining. *Math Med Biol* 2005;22:265–288.
49. Braun RJ, King-Smith PE. Model problems for the tear film in a blink cycle: single-equation models. *J Fluid Mech* 2007;586:465–490.
50. Jones MB, Fulford GR, Please CP, McElwain DLS, Collins MJ. Elastohydrodynamics of the eyelid wiper. *Bull Math Biol* 2008;70:323–343.
51. Doane MG. Blinking and the mechanics of the lacrimal drainage system. *Ophthalmol* 1981;88:844–850.
52. Fatt I. Observations of tear-film break up on model eyes. *Contact Lens Assoc Ophthalmol J* 1991;17:267–281.
53. Sharma A, Tiwari S, Khanna R, Tiffany JM. Hydrodynamics of meniscus-induced thinning of the tear film. *Adv Exp Med Biol* 1998;438:425–431.
54. Braun RJ, Begley C, Winkler A, Nam J, Siddique J. Mathematical modeling of tear break-up based on experimental imaging. *Invest Ophthalmol Vis Sci* 2011;53:554.
55. Liu HX, Begley C, Chen MH, Bradley A, Bonanno J, McNamara NA, et al. A link between tear instability and hyperosmolarity in dry eye. *Invest Ophthalmol Vis Sci* 2009;50:3671–3679.
56. Peng C-C, Cerretani C, Braun RJ, Radke CJ. Evaporation-driven instability of the precorneal tear film. *Adv Colloid Interface Sci* 2013; <http://dx.doi.org/10.1016/j.cis.2013.06.001> [last accessed 12 Nov 2013].
57. Zubkov VS, Breward CJW, Gaffney EA. Coupling fluid and solute dynamics within the ocular surface tear film: a modelling study of black line osmolarity. *Bull Math Biol* 2012;74:2062–2093.
58. Carnahan B, Luther H, Wilkes J. *Applied numerical methods*. New York: John Wiley & Sons; 1969. p 179.
59. Khanal S, Tomlinson A, Diaper CJM. Tear physiology of aqueous deficiency and evaporative dry eye. *Optom Vis Sci* 2009;86:1235–1240.
60. Goto E, Endo K, Suzuki A, Fujikura Y, Matsumoto Y, Tsubota K. Tear evaporation dynamics in normal subjects and subjects with obstructive meibomian gland dysfunction. *Invest Ophthalmol Vis Sci* 2003;44:533–539.
61. Mathers WD, Binarao G, Petroll M. Ocular water evaporation and the dry eye - a new measuring device. *Cornea* 1993;12:335–340.
62. Rolando M, Refojo MF. Tear evaporimeter for measuring water evaporation rate from the tear film under controlled conditions in humans. *Exp Eye Res* 1983;36:25–33.
63. Trees GR, Tomlinson A. Effect of artificial tear solutions and saline on tear film evaporation. *Optom Vis Sci* 1990;67:886–890.
64. Tsubota K, Yamada M. Tear evaporation from the ocular surface. *Invest Ophthalmol Vis Sci* 1992;33:2942–2950.
65. Lemp MA, Crews LA, Bron AJ, Foulks GN, Sullivan BD. Distribution of aqueous-deficient and evaporative dry eye in a clinic-based patient cohort: a retrospective study. *Cornea* 2012;31:472–478.
66. Mainstone JC, Bruce AS, Golding TR. Tear meniscus measurement in the diagnosis of dry eye. *Curr Eye Res* 1996;15:653–661.
67. Creech JL, Do LT, Fatt I, Radke CJ. In vivo tear-film thickness determination and implications for tear-film stability. *Curr Eye Res* 1998;17:1058–1066.
68. Eter N, Gobbels M. A new technique for tear film fluorophotometry. *Br J Ophthalmol* 2002;86:616–619.
69. Fatt I, Weissman BA. *Physiology of the eye: an introduction to the vegetative functions*, 2nd ed. Stoneham, MA: Butterworth-Heinemann; 1992.
70. Forrester JV, Dick AD, McMenamin PG, Lee WR. *The eye: basic sciences in practice*, 2nd ed. Philadelphia: Saunders (Elsevier); 2002.
71. Goto E, Dogru M, Kojima T, Tsubota K. Computer-synthesis of an interference color chart of human tear lipid layer, by a colorimetric approach. *Invest Ophthalmol Vis Sci* 2003;44:4693–4697.
72. Kawakita T, Kawashima M, Murat D, Tsubota K, Shimazaki J. Measurement of fornix depth and area: a novel method of determining the severity of fornix shortening. *Eye* 2009;23:1115–1119.

73. Ehlers N. The precorneal film: biomicroscopical, histological and chemical investigations. *Acta Ophthalmol* 1965;(Suppl. 81):1-136.
74. Tiffany JM, Winter N, Bliss G. Tear film stability and tear surface tension. *Curr Eye Res* 1989;8:507-515.
75. Hodges R, Dartt DA. Keratoconjunctivitis sicca: physiology and biochemistry of the tear film. In: Foster C, Azar D, Dohlman CH, editors. *Smolin and thoft's the cornea: scientific foundations and clinical practice*; 2004. Philadelphia, PA: Lippincott Williams & Wilkins. p 591.

### Supplementary material available online

- Appendix A. Geometries
- Appendix B. Water and salt balances
- Appendix C. Solution methodology
- Appendix D. Estimation of tear flow and lacrimal supply
- Appendix E. Additional tear-dynamics predictions

Supplementary material can be viewed and downloaded at <http://informahealthcare.com/cey>